JJMIE

Volume 19, Number 1, March. 2025
ISSN 1995-6665
Pages 129 – 146
https://doi.org/10.59038/jjmie/190109
Editor-in-Chief: Prof. Ali M. Jawarneh

Jordan Journal of Mechanical and Industrial Engineering

Influence of Concentration and Particle Size of Yellow Oil Fly Ash on Thermal and Mechanical Properties of High-Density Polyethylene

Saif S. Irhayyim*, Farouk M. Mahdi, Saad R. Ahmed

Mechanical Department, College of Engineering, Tikrit University, Iraq.

Received 8 Sep 2024 *Accepted 25 Nov 2024*

Abstract

Developing advanced composite materials is critical for various industrial applications, including automotive, construction, and packaging, where enhanced mechanical and thermal properties are required. This study investigates the thermal and mechanical performance of high-density polyethylene (HDPE) composites reinforced with yellow oil fly ash (YOFA), a by-product of heavy fuel oil. Using injection molding, composites were fabricated with varying concentrations and particle sizes of YOFA. The composites were performed with YOFA particle increments from 0 to 8 wt.%. Mechanical properties were evaluated via tensile, flexural, and Izod impact tests, while thermal properties were examined using thermogravimetric analysis (TGA) and differential thermal analysis (DTA). Energy-dispersive X-ray (EDX) and scanning electron microscopy (SEM) analyses provided insights into the morphology and distribution of YOFA within the composites. Results demonstrated that composites with 2 wt.% YOFA and particle sizes of 53-80 µm exhibited optimal tensile and flexural performance, while impact strength decreased with increasing YOFA content and particle size. Thermal stability was highest for composites with 2 wt.% YOFA and the smallest particle size. SEM images revealed thorough encapsulation of YOFA particles within the HDPE matrix, suggesting effective reinforcement. This study presents a novel approach to enhancing HDPE properties using YOFA particles and contributing to waste valorization.

Keywords: HDPE, oil fly ash, mechanical properties, tensile properties, thermal properties.

1. Introduction

Polymer matrix composites, incorporating reinforcing particles, fibers, or fabrics, have demonstrated superior stability and physical properties, significantly enhancing the strength of composite systems. Predominantly derived from thermoplastics, these composites are preferred for numerous applications [1], [2], [3]. Reinforcing elements include carbon particles, glass fibers, carbon fiber, and cellulose fibers, while nanoparticles like carbon nanotubes and graphene have garnered significant interest for reinforcement in composites. These high-strength composites have promising applications across the aerospace, automotive, construction, and electronics sectors [4], [5]. Today, the world faces severe environmental challenges due to the excessive disposal of waste, which causes significant harm to the environment and poses risks to human health. EU companies could save approximately 600 billion euros by reusing and recycling waste, potentially reducing gas emissions by up to 4% annually [6], [7], [8]. While driving economic growth and urban development, industrial expansion generates non-disposable waste. The increasing demand for electricity in residential and industrial settings is expected to elevate thermal power production and the generation of byproducts like fly ash (FA) [9], [10]. FA, a byproduct from various heavy manufacturing facilities such as oil, cement, and coal-driven power plants, presents disposal challenges but also holds the potential for creating commercially valuable products. Integrating FA into construction materials can yield high-quality, cost-effective products, such as pre-mixed materials for construction sites. Ensuring that the concentration of FA as a filler remains below a specified threshold mitigates the risk of microparticle release due to abrasion [4], [11], [12]. Utilizing FA with cementitious materials extends beyond construction to include polymer composites. Researchers have identified significant interfacial compatibility between FA and plastics, making them suitable for fabricating composites [4], [11]. FA has achieved attention as a superior filler material for polymers because of its highly dispersible, dense, and flowability of spherical particles. FA polymer composites, recognized for their exceptional performance, address environmental concerns and simplify disposal challenges associated with heavy industry FA production [4], [12], [13]. Sreekanth et al. [14] observed that the mechanical characteristics of

* Corresponding author e-mail: saiof11@tu.edu.iq.

particulate-filled polymer composites are affected by the distribution, shape, size, and adhesion of filler particles in the polymer matrix, as well as the crystallization and degree of crystallinity of the semi-crystalline polymer [15]. Recent studies have confirmed the compatibility between FA and plastics, making them suitable for producing composite materials. The inherent ceramic properties of FA particles enhance the physical and mechanical properties of the resulting composites, making them viable for various applications [16], [17]. Plastic-based products are indispensable due to their affordability, lightweight nature, exceptional durability, and resistance to corrosion and weathering. Despite their benefits, single-use plastic products contribute significantly to environmental pollution, affecting water, soil, and human health [6]. Various types of plastic, including polypropylene (PP), polyethylene (PE), and polyamides (PA), are available. High-density polyethylene (HDPE), a thermoplastic polymer known for its high stability, finds extensive use in packaging, automotive components, building materials, and electronics. HDPE is a semicrystalline plastic that exhibits strong mechanical properties and is resistant to moisture and chemicals [4], [18], [19], [20].

Numerous research has concentrated on assessing how FA affects the mechanical properties of HDPE. Most of these studies have examined using coal and oil FA to reinforce HDPE to create PMCs. For instance, Ahmad et al.[21] investigated the mechanical properties of HDPE reinforced with coal FA. The study utilized three different types of FA particle sizes and varied the concentration of FA up to 40% by weight. The results showed that both flexural and tensile strengths, as well as moduli, increased with the addition of FA. However, the tensile elongation significantly decreased when the FA concentration exceeded 10%. Impact resistance decreased with increasing FA concentration by up to about 15% but did not show a significant reduction with further addition. Additionally, composites containing the smallest FA particles were the most effective in enhancing strength and relative elongation. Interestingly, the particle size did not significantly influence the modulus and impact resistance. Alghamdi[17]investigated the influence of filler particle size on the recyclability and mechanical properties of oil FA-reinforced HDPE composites. The research focused on creating and analyzing composites of HDPE matrices. It revealed that incorporating small (50–90 μm) FA particles significantly enhanced the tensile modulus (by approximately 95%) and tensile strength (by around 7%) of the reinforced composites than pure HDPE materials. However, when the composites were recycled multiple times using an extrusion-based process, the mechanical properties slightly decreased, mainly due to the separation of the filler and matrix when larger FA particles were utilized. Despite this, the recycled composites' tensile modulus and tensile strength with small FA particles remained considerably higher than those of pure HDPE materials. Alghamdi [4] investigated the impact of 5, 10, and 15 wt.% oil FA on HDPE matrix composites and studied its thermal, morphological, and tensile properties. The analysis using thermogravimetric (TGA) tests revealed that the composites have a highly uniform distribution of fillers. Adding 15 wt.% FA significantly increased Young’s modulus by approximately 200% compared to pure HDPE polymer without compromising the tensile strength. To assess the durability of the composites, samples were subjected to environmental aging involving UV and moisture exposure, and their morphological and mechanical properties were evaluated. The study concluded that the FA/HDPE composites are more suitable for long-term use than pure HDPE. A 10 wt.% FA content was observed to be more effective in maintaining tensile strength after 20 weeks of aging. However, when considering both tensile strength and Young’s modulus, the composite with 15 wt.% FA performed the best. Even after 20 weeks of aging, this composite only exhibited a ~5% decline in Young’s modulus and a ~9% decline in tensile strength compared to its freshly made counterpart. The remarkable capacity of densely concentrated FA to capture high-energy photons from UV light prevents the degradation of the polymer matrix caused by the photons, making the material ideal for extended outdoor applications.

Previous studies have primarily focused on using coal and black oil fly ash (FA) to reinforce high-density polyethylene (HDPE). However, the characteristics of HDPE reinforced with a novel type of FA, known as yellow-oil FA (YOFA) particles, have not been thoroughly investigated. YOFA is a byproduct from thermal power stations that use heavy fuel oil treated with magnesium oxide (MgO). This study aims to fill this knowledge gap by extensively examining HDPE-YOFA composites. The findings could enable the use of these composites in critical aerospace and automotive components, potentially revolutionizing these industries. Additionally, this research provides a comprehensive analysis of the thermal and mechanical properties of HDPE-YOFA composites under normal operating conditions using both qualitative and quantitative methods. Expanding the scope beyond traditional coal and black oil FA, this study introduces an innovative approach to reinforcing HDPE composites, significantly contributing to the current knowledge base.

2. Materials and methods

2.1. Materials

The high-density polyethylene (HDPE) utilized is a thermoplastic (Grade: SABIC HDPE B5429) purchased from Saudi Basic Industries Corporation (SABIC) in Riyadh, Saudi Arabia. The HDPE granules have specific properties obtained from the source: a rate of melt flow (MFR) of 0.3 g/10 min at 190 °C/2.16 kg (ASTM D1238), a Vicat softening temperature of 124 °C (ASTM D1525), a density of 0.954 g/cc at 23 °C (ASTM D1505), and a brittleness temperature of <-75 °C (ASTM D746). Samples of YOFA were obtained from the Al-Qayyarah power station in Nineveh, Iraq. This power station utilized heavy fuel oil treated with magnesium oxide (MgO) to extend the durability of steel components like boiler tubes and turbine blades, which are used with gaseous fuels (residual fuel). The MgO interacts with vanadium in the fuel oil to reduce corrosion and uphold the operational reliability of the turbines. The YOFA samples were collected directly from the sites where heavy fuel is burned to produce electricity. They were collected as coarse particles from the station's mechanical hoppers and used naturally without chemical

or physical processing. These samples were then combined and homogenized using suitable coning and quartering techniques. Approximately 3 kg of YOFA was collected from various places, and all the samples were blended to form a final mixture for conducting extraction experiments. The YOFA is a bright yellow substance with a density of 2.18 g/cc. The YOFA particle density was measured according to ASTM D2320 (Pycnometer method) [22].Energy-dispersive X-ray spectrometry (EDX) and scanning electron microscopy (SEM) were employed to capture detailed, high-magnification images to examine their morphological characteristics. Figure shows SEM images and EDX analysis of YOFA particles of different sizes: YOFA 1, YOFA 2, YOFA 3, and YOFA 4, respectively. The SEM images clearly reveal the dendritic and irregular shapes of the YOFA particles, providing insights into their dimensions. Furthermore, the EDX analysis data indicates that the YOFA particles exhibit high concentrations of carbon (C), oxygen (O), magnesium (Mg), sulfur (S), and vanadium (V). These findings highlight the complex composition and unique morphology of YOFA particles, which are crucial for understanding their reinforcing potential in HDPE composites.

Furthermore, the total organic content (TOC) in a YOFA sample, which refers to the amount of organic material present, was analyzed using ELTRACW multiphase CO_2/H_2O determination. The chemical composition of the YOFA, as shown in Table 1, was analyzed utilizing a Shimadzu sequential X-ray fluorescence (XRF-1800) spectrometer manufactured in Japan. This instrument utilizes X-ray fluorescence analysis measurements to determine the elemental composition of the YOFA.

Table 1. Chemical composition of YOFA.

Oxide composition		Elemental composition	
Component	**wt. %**	**Component**	**ppm**
Al_2O_3	0.095	S	302461
Fe_2O_3	2.869	Co	588
CaO	0.488	Cr	3339
MgO	18.761	Cu	25
Na_2O	0.074	Mo	56
TiO_2	0.041	Ni	32905
MnO	0.044	Sr	44
P_2O_5	0.131	V	22626
SO_3	25.5	Zn	507
TOC	7.47	Zr	46
LOI	8.27	La	13
-	-	Pb	21

2.2. Preparation of composites

The YOFA powders were initially ground using an electrical powder grinder at a speed of 25000 r.p.m for 15 minutes. This process was carried out to create a wide range of particle sizes. The resulting powder was then sieve-screened to produce four different sizes based on particle size: YOFA 1 (53-80 µm), YOFA 2 (80-125 µm), YOFA 3 (125-150 µm), and YOFA 4 (150-250 µm). The HDPE and YOFA underwent an 8-hour drying process at 80°C to eliminate moisture and volatile substances. Prior to the melt blending (extrusion) procedure, the YOFA and HDPE were mixed manually with an acetone solvent to facilitate improved dispersion of YOFA within the HDPE matrix. As Verma et al.[23] suggested, the YOFA particles adhere to the surface of HDPE granules due to the acetone solvent's presence. Preparing HDPE/YOFA composites involved obtaining a mixed filament through melt blending using a single-screw extruder-type SJ25 plastic extruder. The extruder was configured with a screw of 25 mm diameter and an L/D ratio of 16. The temperature was controlled at 40°C, 150°C, and 140°C in the first, second, and third zones, correspondingly, from the feeding zone to the mold exit. The screw speed ranged from 9 to 11 r.p.m. Four different mixtures of HDPE/YOFA composites were separately prepared by incorporating YOFA particles in increments of 2%, varying from 0 to 8 wt.%, for each YOFA particle size. After the process of extrusion, the filament mixture was cut using an electric cutter to form granules. These granules were then shaped into test specimens using a vertical plastic injection molding machine XCX-40G, following a preliminary study to determine the typical parameters as presented in Table 2. Prior to injection molding, all granules of HDPE/YOFA composites were dried for 2-hour at 80°C to remove the moisture leftover from the extrusion process. Figure 2 details the schematic diagram for preparing HDPE/YOFA composites. In Table 3, the samples are identified as HXFY, where X represents the content of YOFA, and Y represents the particle size grades. Additionally, pure HDPE is denoted as NHD.

Table 2. The typical parameters of the injection molding machine.

Typical Parameters	
Injection temperature	160 ºC
Holding temperature time	6-8 min
Injection pressure	0.6 MPa
Holding pressure time	30 s
Injection time	1 s
Mold temperature	23±2 ºC
Cooling time	1-2 min

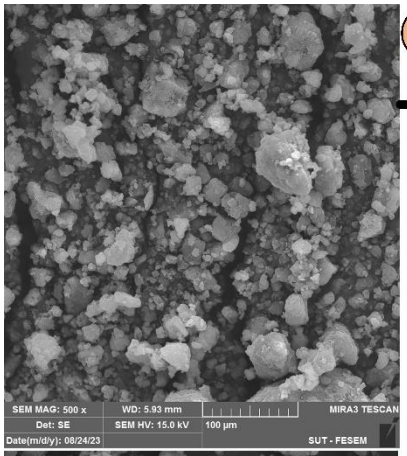

YOFA 1

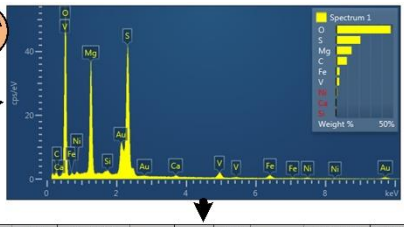

Element	Line Type	Apparent Concentration	K Ratio	Wt.%	Wt.% Sigma	Atomic %	Standard Label	Factory Standard
C	K series	0.34	0.00337	9.49	0.57	15.32	C Vit	Yes
O	K series	15.09	0.05079	47.78	0.39	57.93	SiO2	Yes
Mg	K series	4.41	0.02927	13.59	0.15	10.85	MgO	Yes
Si	K series	0.14	0.00113	0.43	0.05	0.30	SiO2	Yes
S	K series	6.87	0.05914	21.29	0.21	12.88	FeS2	Yes
Ca	K series	0.15	0.00133	0.45	0.06	0.22	Wollastonite	Yes
V	K series	0.78	0.00782	2.84	0.11	1.08	V	Yes
Fe	K series	0.86	0.00860	3.06	0.16	1.06	Fe	Yes
Ni	K series	0.30	0.00304	1.08	0.18	0.36	Ni	Yes
Total:				100.00		100.00		

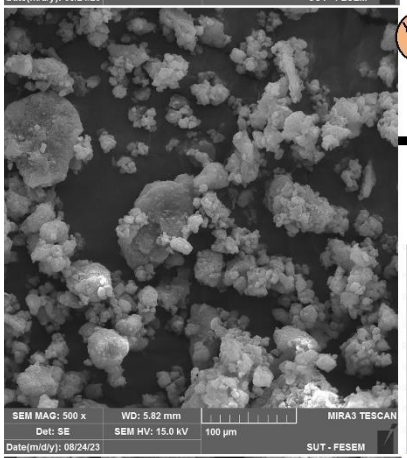

YOFA 2

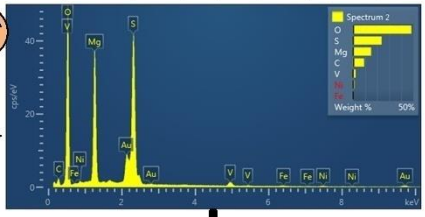

Element	Line Type	Apparent Concentration	k Ratio	Wt.%	Wt% Sigma	Atomic %	Standard Label	Factory Standard
C	K series	0.41	0.00405	10.75	0.51	15.94	C Vit	Yes
O	K series	12.6	0.04240	48.40	0.36	58.85	SiO2	Yes
Mg	K series	4.46	0.02959	11.3	0.22	9.52	MgO	Yes
S	K series	6.87	0.05914	21.29	0.21	12.88	FeS2	Yes
V	K series	2.09	0.02090	6.58	0.17	2.30	V	Yes
Fe	K series	0.13	0.00134	0.41	0.11	0.13	Fe	Yes
Ni	K series	0.41	0.00412	1.27	0.16	0.38	Ni	Yes
Total:				100.00		100.00		

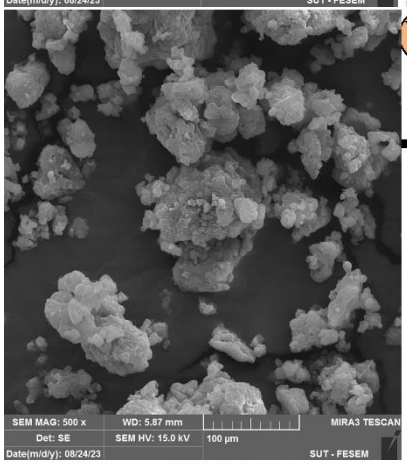

YOFA 3

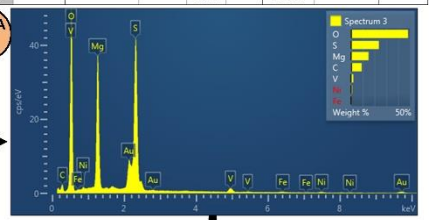

Element	Line Type	Apparent Concentration	K Ratio	Wt.%	Wt.% Sigma	Atomic %	Standard Label	Factory Standard
C	K series	0.27	0.00271	9.13	0.50	14.59	C Vit	Yes
O	K series	13.88	0.04670	48.38	0.36	58.04	SiO2	Yes
Mg	K series	4.48	0.02970	14.95	0.15	11.80	MgO	Yes
S	K series	6.90	0.05940	23.74	0.21	14.21	FeS2	Yes
V	K series	0.52	0.00518	2.10	0.11	0.79	V	Yes
Fe	K series	0.14	0.00139	0.55	0.13	0.19	Fe	Yes
Ni	K series	0.29	0.00290	1.15	0.18	0.37	Ni	Yes
Total:				100.00		100.00		

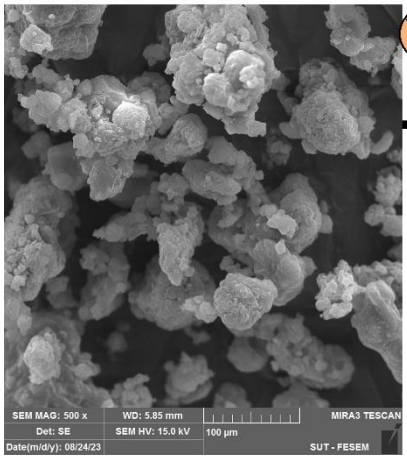

YOFA 4

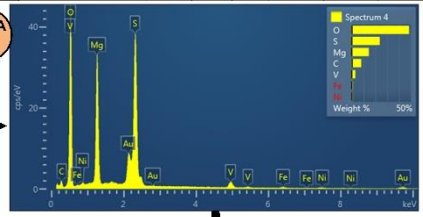

Element	Line Type	Apparent Concentration	K Ratio	Wt.%	Wt.% Sigma	Atomic %	Standard Label	Factory Standard
C	K series	0.22	0.00225	8.16	0.49	13.22	C Vit	Yes
O	K series	12.60	0.04240	48.40	0.36	58.85	SiO2	Yes
Mg	K series	3.99	0.02647	14.53	0.14	11.63	MgO	Yes
S	K series	6.38	0.05498	23.75	0.22	14.41	FeS2	Yes
V	K series	0.71	0.00711	3.12	0.12	1.19	V	Yes
Fe	K series	0.24	0.00244	1.05	0.14	0.37	Fe	Yes
Ni	K series	0.23	0.00230	0.98	0.19	0.33	Ni	Yes
Total:				100.00		100.00		

Figure 1. SEM image and elemental content (EDX) for YOFA 1, YOFA 2, YOFA 3, and YOFA 4.

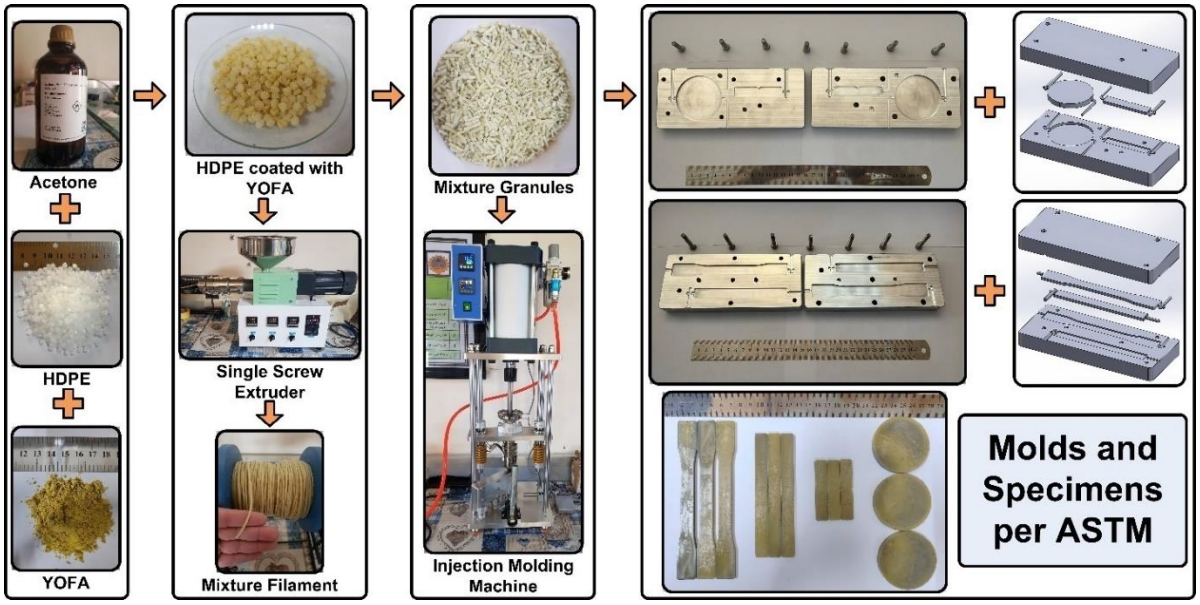

Figure 2. The schematic diagram for the preparation of HDPE/YOFA composites.

Table 3. The sample labels at different particle size grades and YOFA content.

YOFA (wt.%)	YOFA 1 (53-80 µm)	YOFA 2 (80-125 µm)	YOFA 3 (125-150 µm)	YOFA 4 (150-250 µm)
0	NHD	NHD	NHD	NHD
2	H2F1	H2F2	H2F3	H2F4
4	H4F1	H4F2	H4F3	H4F4
6	H6F1	H6F2	H6F3	H6F4
8	H8F1	H8F2	H8F3	H8F4

2.3. Mechanical properties:

The mechanical properties were tested under standard conditions of 50±2% relative humidity and 23±2°C. The data provided in the current study represent the average outcomes derived from three samples for each test, accompanied by the related standard deviations. Figure 3 shows the standard specimens of the mechanical properties used in the present study according to ASTM standards.

2.3.1. Tensile properties:

The tensile properties of the HDPE/YOFA composite, including yield strength, tensile strength, tensile modulus, and elongation at break, were determined following the ASTM D638 standard for dog-bone-shaped specimens (Type I) [24]. The experimental data was obtained using a 50 mm gauge length and a crosshead speed of 50 mm/min on a Universal Testing Machine (UTM) manufactured by LARYEE in China. The tensile elastic modulus was determined by analyzing the linear portion of the load-extension curve and calculating its slope. The yield stress was identified by locating the endpoints of the linear region of the load-extension curve. Tensile strength was derived from the peak stress reached during the test. Lastly, the elongation at break was determined by identifying the point at which the stress dropped to zero during the test [25].

2.3.2. Flexural properties:

The flexural properties, encompassing flexural strength and modulus, were assessed following ASTM D790 [26].The measurements used a gauge length of 80 mm and a crosshead speed of 1.5 mm/min, employing the LARYEE UTM from China.

2.3.3. Impact properties:

The notched Izod impact strength of the HDPE/YOFA composite specimens underwent evaluation utilizing an Impactometer from Time Group, China, following the ASTM D256 guidelines [27]. The standardized test procedure involved assessing the Izod ASTM pendulum impact resistance of plastics with a 2.54 mm notch depth, a 5.5 J hammer, and a 45º angle notch. The strength of the notched Izod impact was determined using the following Equation[28]:

$$\textbf{Izod impact strength } (\mathbf{KJ/m^2}) = \left(\frac{\mathbf{E}}{\mathbf{d \times h}}\right) \times \mathbf{10^3} \quad (1)$$

Where E represents the corrected energy in J that is absorbed by breaking the test sample, the variable d represents the thickness of the test specimen in mm. In contrast, h represents the width remaining at the notch base of the test sample in mm.

2.4. Thermal properties

The study involved conducting thermogravimetric analysis (TGA) to measure the simultaneous weight change and differential thermogravimetric analysis (DTA) to record the maximum degradation temperatures. These analyses were conducted using an SDT Q600 V20.9 Build 20 thermal analyzer instrument with a heating rate of 20 °C/min across a temperature range of 25–800°C under a flowing Argon atmosphere. Specifically, TGA and DTA were employed to investigate the thermal stability of HDPE and HDPE/YOFA composites by determining the initial, final, and maximum degradation temperatures, as well as the corresponding percentage weight loss for the composites.

3. Results and discussion

3.1. Tensile properties

The most critical tensile mechanical properties of polymeric materials include yield strength, tensile strength, tensile modulus, and elongation at break. The mechanical properties of composite materials are predominantly affected by including a filler and any alterations made. Composites can exhibit superior mechanical properties when the filler is effectively distributed throughout the matrix [29], [30]. Besides, the mechanical properties are influenced by several factors, such as the type and concentration of filler, mixing conditions, filler shape, particle size distribution, and the bonding between matrix and filler [31]. The ingredients are identical and manufactured under consistent process conditions, which ensures uniform material properties, randomness, bond strength, phases, and shape. As a result, the characteristics of the interface, including its nature, strength, proportion, size, and distribution, play a significant role in determining the resulting properties.Figure **4**,Figure **5**,Figure **6**, andFigure **7** demonstrate the influence of different weight fractions of YOFA particles on the yield strength, tensile strength, tensile modulus,and elongation at break, respectively, of both the virgin HDPE and HDPE/YOFA composites at various particle size grades. As can be observed, the yield strength, tensile strength, and tensile modulus results improved significantly by increasing the YOFA particle content up to 2 wt.% of the HDPE matrix composite, especially at the smallest particle size (YOFA 1) and gradually decreasing for all the composites. The smallest YOFA particle size composites have yield and tensile strengths higher than neat HDPE up to 4 wt.% YOFA content. In contrast, the elongation at break has the contrasting trend behavior mentioned above, which considerably declined up to 2 wt.% and then marginally increased. Moreover, the yield strength, tensile strength, and tensile modulus significantly declined as the YOFA particle size increased, while the elongation at break gradually increased with increasing particle size.

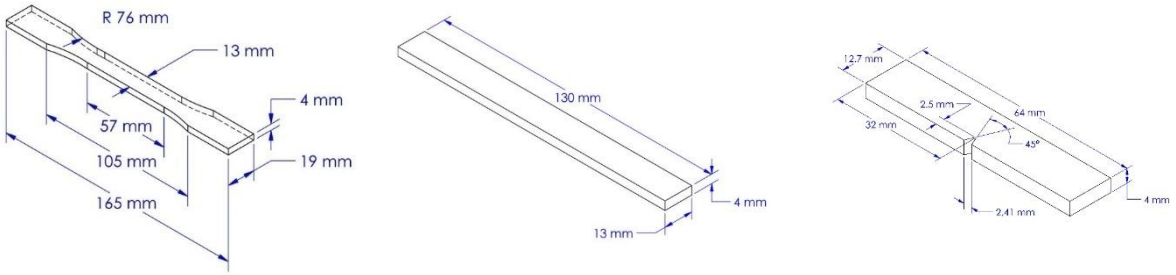

(A) (B) (C)

Figure 3. Standard samples of the mechanical properties according to ASTM standards: (A) Tensile sample, (B) Flexural sample, (C) Impact sample.

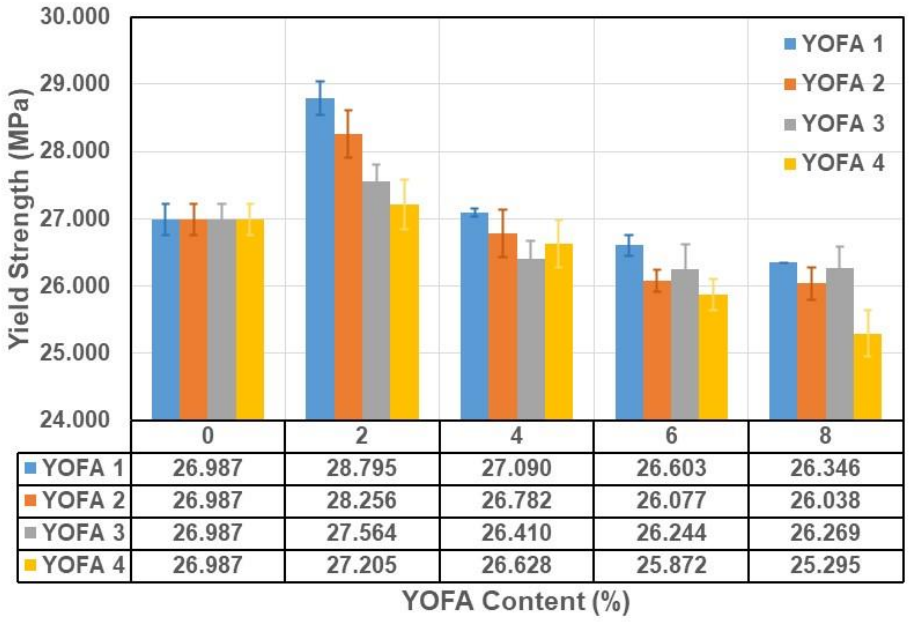

	0	2	4	6	8
YOFA 1	26.987	28.795	27.090	26.603	26.346
YOFA 2	26.987	28.256	26.782	26.077	26.038
YOFA 3	26.987	27.564	26.410	26.244	26.269
YOFA 4	26.987	27.205	26.628	25.872	25.295

Figure 4. Correlation between the yield strength with the content and particle size of YOFA content.

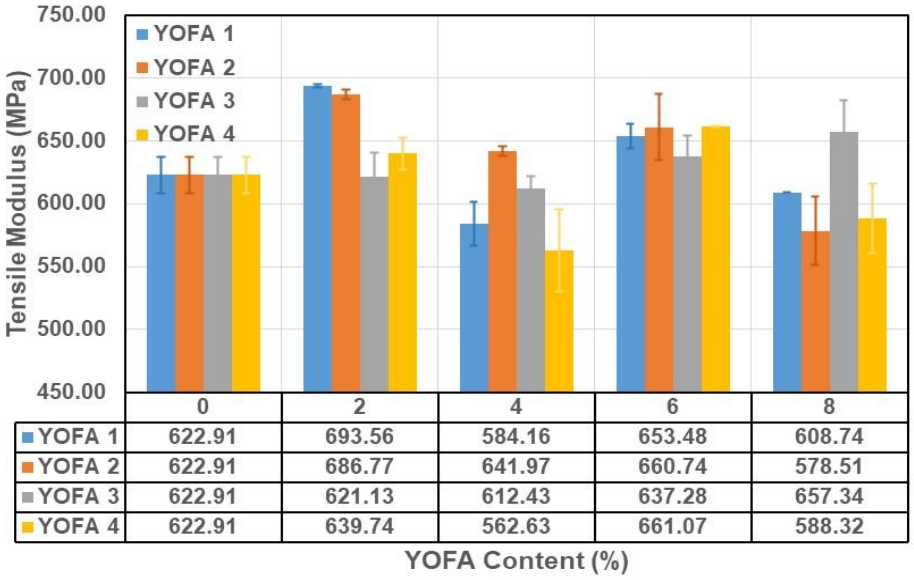

	0	2	4	6	8
YOFA 1	622.91	693.56	584.16	653.48	608.74
YOFA 2	622.91	686.77	641.97	660.74	578.51
YOFA 3	622.91	621.13	612.43	637.28	657.34
YOFA 4	622.91	639.74	562.63	661.07	588.32

Figure 5. Correlation between the tensile modulus with the content and particle size of YOFA content.

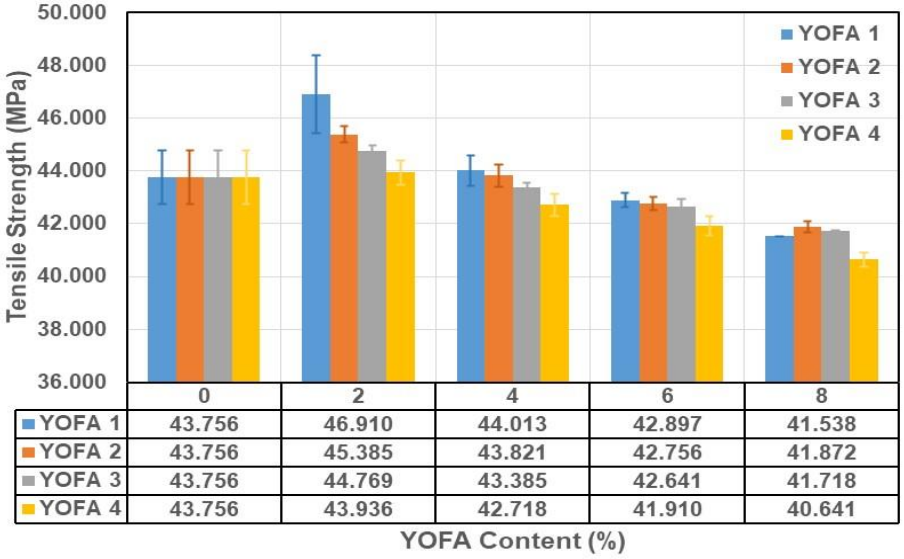

	0	2	4	6	8
YOFA 1	43.756	46.910	44.013	42.897	41.538
YOFA 2	43.756	45.385	43.821	42.756	41.872
YOFA 3	43.756	44.769	43.385	42.641	41.718
YOFA 4	43.756	43.936	42.718	41.910	40.641

Figure 6. Correlation between the tensile strength with the content and particle size of YOFA content.

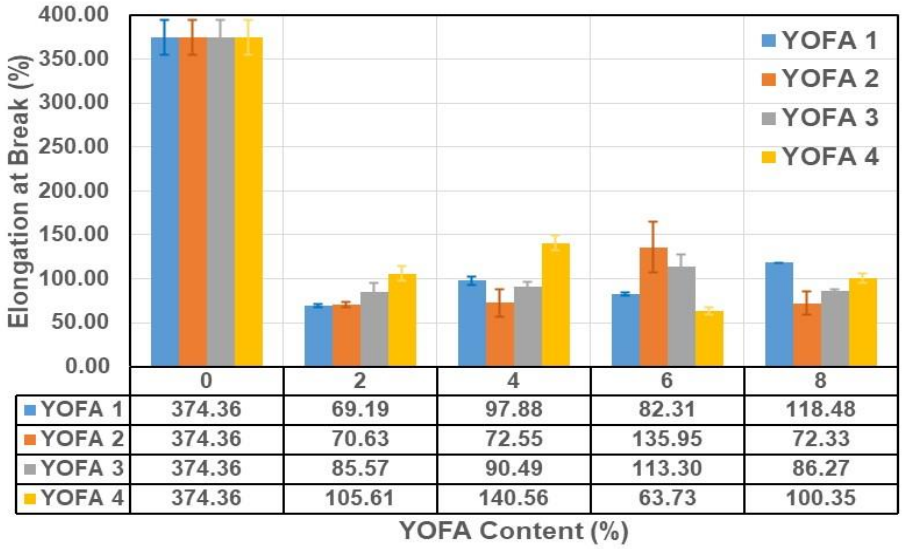

	0	2	4	6	8
YOFA 1	374.36	69.19	97.88	82.31	118.48
YOFA 2	374.36	70.63	72.55	135.95	72.33
YOFA 3	374.36	85.57	90.49	113.30	86.27
YOFA 4	374.36	105.61	140.56	63.73	100.35

Figure 7. Correlation between the elongation at break with the content and particle size of YOFA content.

These findings indicate that pure HDPE is the most ductile sample, hinting at the reinforcement of the YOFA particles. HDPE is characterized by a semicrystalline structure comprising spheroidal aggregates of crystals embedded within a continuous amorphous phase. Figure 8 provides a detailed view of the SEM images of the fractured tensile surface of neat HDPE (NHD). At low magnification, the images display a relatively homogeneous fracture surface, suggesting a ductile failure mode characterized by the presence of significant plastic deformation. Under higher magnification, the micrographs reveal a fibrous structure with long fibrils aligned along the direction of tension. This fibrillation pattern is characteristic of flexible polymers and suggests significant plastic deformation before fracture. The fibrils seem connected, creating a network that offers a valuable understanding of how HDPE absorbs energy during tensile stress. Upon closer inspection, tiny voids and small indentations scattered were observed throughout the fractured surface. These characteristics are typical of a ductile fracture mechanism, where the merging and expansion of these tiny voids contribute to the eventual failure of the material. The uniform size and shape of the indentations further support the idea of a ductile fracture. In some regions, the micrographs show the localized thinning of the material and the development of shear bands, indicating areas of concentrated stress and shear deformation. These features suggest the initiation and spread of cracks under tensile stress, ultimately leading to the material's breakdown. The observed microstructural characteristics, such as fibrillation, microvoids, and dimples, align with the well-known ductile behavior of HDPE under tensile loading. This detailed analysis is a key part of our research, providing valuable insights into the behavior of HDPE under tensile stress.

The load-bearing characteristics are contingent upon the efficient transmission of loads from the encompassing matrix to the filler particles. The mechanism of toughening the tensile strength of particulate-reinforced polymers, as shown in Figure 9, is well understood and can be divided into three stages[25], [32], [33]:

1. Stress concentration: When a rigid dispersant and a ductile polymer are combined, the difference in stiffness between the two materials can cause stress to concentrate in the composite material.
2. Debonding: When a tensile force is applied, the interfaces between the dispersant and the polymer debond, leading to the creation of voids, the formation of ligaments, and crazing.
3. Cavitation: In this final stage, continued tension causes shear yielding, further extending the voids, ligaments, and crazing. This process enhances the material's strength and stiffness, providing a notable advantage. However, it is crucial to acknowledge that it also serves as a precursor to brittle failure, which constitutes a potential drawback worth considering. This understanding is crucial for us as materials engineers and researchers in the field of polymer science.

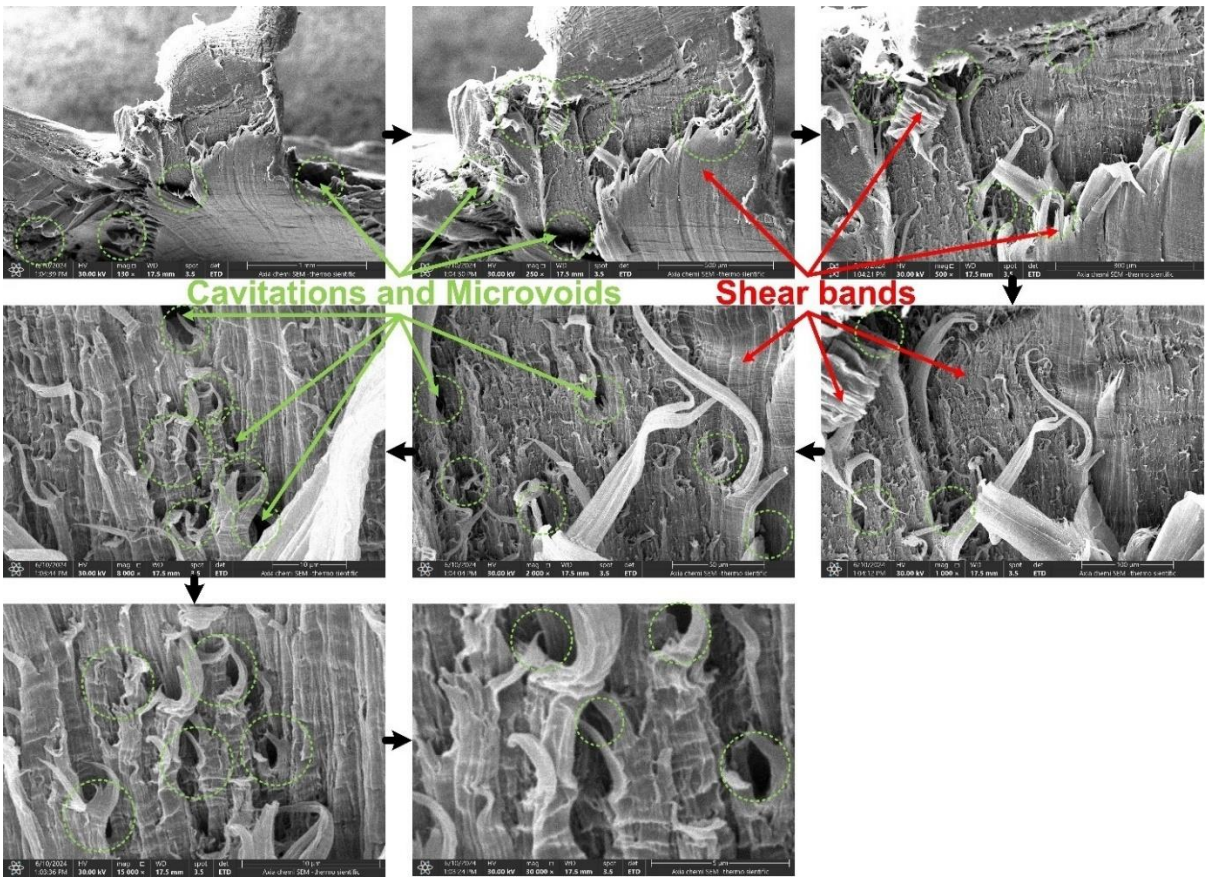

Figure 8. SEM images of the fractured surfaces of the NHD specimen broken in a tensile test.

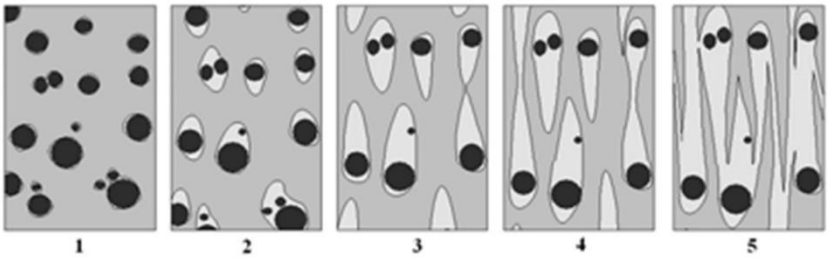

Figure 9. Schematic presentation of steps concerned with tensile fracture [21].

The increase in YOFA concentration led to a higher tensile modulus. This finding supports an earlier study by Ahmad et al. [21], which suggested that the strength of the interaction has minimal influence on the modulus. The high modulus of the composite material can be attributed to the relationship between the modulus and small strain values. The application of small strain values generates corresponding small stresses, which are insufficient to disrupt the weak interactions at the interface. Consequently, these small stresses facilitate an effective transfer of mechanical load from the matrix to the filler, enabling the filler to bestow its high modulus property upon the composite.

The increase in tensile properties up to 2 wt.% YOFA content can be related to the formation of strong interactions between the matrix and the filler, leading to improved tensile properties compared to the pure polymer. This is believed to occur because the hydrophobic ends of YOFA particles on the surface were adsorbed onto the polymer surface, creating robust interfacial interactions. These interactions serve to limit the mobility of the polymer chains and reduce the effects of stress concentration, thereby improving the overall tensile strength[28]. Besides, this improvement correlated with the dispersion of hard YOFA particles in a soft matrix, although the particles' stress concentration would moderate this.Moreover, the particles of YOFA have an irregular and dendritic surface shape, which can be observed in Figure 1. This shape results in anenormous contact area and improves the adhesion with the HDPE matrix. The enhanced bonding at the interface reduces the chances of particle pull-out and matrix cracking during tensile testing, ultimately leading to improved tensile properties.Based on the rule-of-mixtures theory, one would anticipate that the stiffness would rise in proportion to the quantity of the tough YOFA phase added, as shown up to 2 wt.% YOFA content. After that, the pattern with increasing levels of YOFA addition implies that another important factor is likely at play, such as an escalating stress concentration from the YOFA particles. With increasing YOFA concentration up to 8 wt.%, the increased deformation linked to the larger quantity of the relatively hard phase also points to the potential for embrittlement arising from recrystallization, crazing, or considerable stretching and reduction in the width of the ligaments [25]. This decrease in tensile properties is likely due to the formation of voids and porose due to separation and the formation of air bubbles during testing. These issues are caused by the large amounts of hard dispersants, which create thinner and weaker connections within the material. Likewise, the decline in tensile properties can be correlated with an increase in filler concentration, with no specific interaction occurring between HDPE and YOFA [29]. Besides, this reduction in elongation at break and tensile strength has previously been attributed to stress concentrations that cause cracks to form around filler particles, as explained by Atikler et al.[31] and Satapathy et al.[34]. The significant decline in the elongation at break is attributed to the rigid YOFA particles, which limit the polymer matrix's flexibility.The elongation at break values decreased significantly as the YOFA loading increased. Bose and Mahanwar [35] explained the drastic decline in elongation at break in FA/Nylon 6 composites due to the filler's wide particle size distribution. Smaller particles might have occupied the interstitial volume at high filler content, resulting in an insufficient matrix available to contribute to the elongation percentage.

On the other hand, the tensile properties exhibited a negative correlation with the increasing particle size of YOFA for all concentrations. When the particle size of YOFA rose, the tensile properties declined slightly and gradually. The size and distribution of YOFA particles within the HDPE matrix play a vital role in determining the composite's tensile properties. The main reason for the deterioration of the tensile properties with increasing particle size of the YOFA content is attributed to the lower surface area-to-volume ratio. Consequently, they offer fewer points of contact for bonding with the HDPE matrix, which results in diminished interfacial adhesion and less mechanical properties of the composite. Furthermore, when particles in a material are too large, or there is an excessive amount of them, this can have a negative impact on the material's tensile properties. This occurs because larger particles may not be effectively bonded to the matrix, and an increased particle content can lead to agglomeration, disrupting the matrix's continuity. The bond strength between YOFA particles and the HDPE matrix is crucial in determining the material's tensile strength. As the particle size increases, the available surface area for bonding decreases in relation to the volume, potentially resulting in a weaker bond strength between the matrix and the particles, ultimately reducing its strength. Besides, the effective load transfer from the HDPE matrix to the YOFA particles significantly influences the tensile strength. If the YOFA particles are larger and more numerous, they might hinder this process by acting as stress concentrators instead of stress distributors, especially if there is insufficient interfacial adhesion. Larger YOFA particles can create localized stress concentrations, leading to an uneven distribution of stress that does not contribute to the strength of the composite material. The concept of thermal mismatch involves the variations in thermal expansion coefficients between HDPE and YOFA. These differences lead to internal stresses due to temperature fluctuations. The presence of larger particles exacerbates this issue due to

their size, potentially leading to micro-cracking and a reduction in strength.

Figure 10 and Figure **11**depict SEM images of the fractured surfaces of the tensile sample of H2F1 and H8F1, respectively, which indicate the relatively optimal conditions of tensile properties. In contrast, Figure 12 and Figure **13** show the SEM images of the fractured surfaces of the tensile sample of H2F4 and H8F4, respectively, which reveal lower conditions of tensile properties. The SEM analysis of fractured tensile surfaces provides valuable insights into the fracture mechanisms and the influence of YOFA content on the mechanical properties of HDPE composites. The SEM images showed that voids formed at the YOFA and matrix interfaces. As these voids elongated, they merged and caused fracture or breakage. Thereby, the concentration of voids increased with the concentration of YOFA. The SEM image provided insight into the tensile failure mechanism, which is illustrated in Figure 9. The best tensile properties are observed with 2 wt.% YOFA reinforcement at lower particle size, attributed to the even dispersion and effective stress transfer facilitated by smaller particle size. On the other hand, 8 wt.% reinforcement leads to relatively lower tensile properties due to particle agglomeration and poor interfacial adhesion. These findings emphasize the significance of optimizing YOFA content and particle size to enhance the mechanical properties of HDPE matrix composites. The SEM micrographs of the fractured tensile surfaces of H2F1, as displayed in Figure 10, show that the material experienced a ductile fracture mechanism with extensive plastic deformation. On the fracture surface, there is a fibrillar morphology with elongated fibrils aligned along the direction of the applied tensile stress. These fibrils are interconnected, forming a cohesive network that indicates effective transfer of loading between the YOFA particles and the HDPE matrix. The images display uniformly dispersed YOFA particles at higher magnifications with minimal agglomeration. These YOFA particles are well-embedded within the HDPE matrix, contributing to the improved mechanical properties observed at this reinforcement level. Furthermore, microvoids and dimples are prevalent across the fracture surface, suggesting a ductile fracture mode facilitated by the presence of YOFA. The size and distribution of these features align with the observed enhancement in strength of tensile and elongation at the fracture point. In contrast, the SEM images of sample H8F1, as depicted in Figure 11, show a fracture surface that appears rough and irregular, with a high concentration of YOFA particles exposed at the surface. The presence of numerous YOFA particles leads to their agglomeration, acting as stress concentrators. This promotes crack initiation and propagation. At higher magnifications, the micrographs observe a significant reduction in fibrillar structures, with fewer and shorter fibrils compared to sample H2F1. Large, poorly bonded YOFA clusters also indicate weak interfacial adhesion between the YOFA particles and the HDPE matrix. This weak bonding results in premature failure, which is reflected in the reduced tensile properties at 8 wt.% YOFA. The comparison of the SEM images shows that the best tensile properties are achieved with 2 wt.% YOFA reinforcement. At this concentration level, the small particle size and even distribution of YOFA help transfer stress effectively and increase ductility. This is evidenced by the fibrous shape and even dimple distribution. The ductile fracture mechanism at 2 wt.% indicates better energy absorption and resistance to crack propagation. On the other hand, using 8 wt.% YOFA reinforcement results in clumping and poor bonding between the particles. The diminished fibrillar structures and the presence of large YOFA clusters correlate with the reduced mechanical performance, emphasizing the adverse effects of excessive YOFA content on the tensile properties of HDPE. Besides, the images obtained through SEM of the fractured tensile surfaces of H2F4, as displayed in Figure 12, reveal a combination of ductile and brittle fracture characteristics. When observed at lower magnifications, the fracture surface appears relatively smooth, with some areas showing plastic deformation. Large YOFA particles are present but seem well-dispersed within the HDPE matrix with little to no agglomeration. At higher magnifications, the micrographs show elongated fibrils and microvoids distributed across the fracture surface. These fibrils indicate localized plastic deformation, suggesting that the large YOFA particles contribute to stress distribution and energy absorption during tensile loading. The microvoids, surrounded by dimples, provide further evidence for the ductile fracture mechanism, which enhances the composite's tensile properties at this level of reinforcement. In contrast, the SEM images of H8F4, as shown in Figure 13, show a fractured surface with a rough and irregular appearance, featuring numerous large YOFA particles that are clearly visible. A high concentration of YOFA leads to significant particle agglomeration, which acts as a stress concentrator and makes it easier for cracks to form and spread. Higher magnification images show that not many fibrillar structures are present, but many large YOFA particles are exposed. This suggests no strong bond between the polymer matrix and the YOFA. The YOFA particles are not firmly attached to the polymer matrix because the fillers have detached from the matrix. This detachment is caused by poor adhesion at the interface between the matrix and the fillers. The low adhesion at the interface results in poor stress transfer from the matrix to the particles, decreasing tensile strength as the fillers increase. The extensive particle agglomeration results in a brittle fracture mode, where there is a lack of significant plastic deformation. These findings align with the reduced tensile properties observed at this higher reinforcement level. Upon examination using SEM images, it was observed that the separation of the matrix material originated primarily at the interface of the larger YOFA particles rather than around the smaller particles. When the specimen is elongated, stress transfers from the polymer to the YOFA through the interface, but this transfer is contingent on the quality of the interfacial bond. Voids were found to form at the YOFA-matrix interface. These voids coalesce when the material is elongated, leading to fractures or breaks. It was noted that the concentration of voids increased with YOFA concentration, ultimately decreasing the elongation at break. Moreover, as the particle size increased, the void size correspondingly increased, consequently leading to premature failure. This phenomenon likely accounts for the diminished relative elongation observed in materials with larger YOFA particle sizes. Additionally, the

enhanced surface area offered by smaller particles may serve as an additional influential factor, facilitating heightened interaction with the matrix polymer.

Kabir et al.[25] and Ahmad et al. [21]noticed a similar trend of increasing the tensile properties of HDPE/FA composites up to 2.5 wt.% and then decreasing them.Similar decreasing behavior in elongation at break and tensile strength has been published in the literature [23], [29], [31], [34], [36], [37], [38], [39]. Besides, Alghamdi [4], [17] also reported similar results while studying the effect of oil FA concentration and particle size on HDPE matrix composites. This revealed that increasing the concentration of the oil FA declined the tensile strength but improved the tensile modulus while increasing the size of particles of the filler declined the tensile strength at yield and tensile modulus.

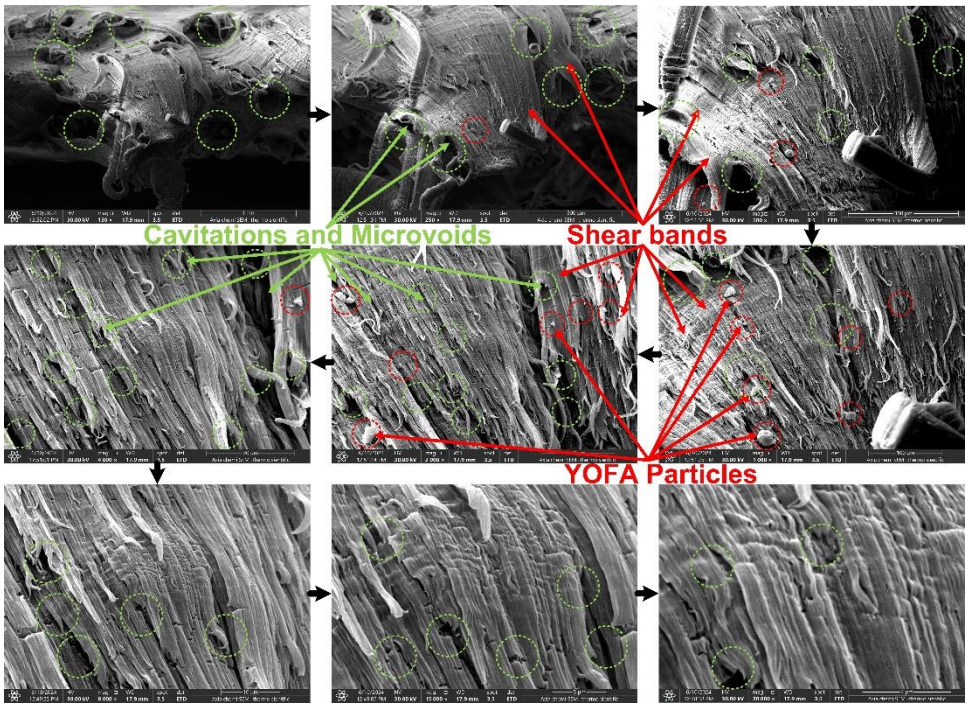

Figure 10. SEM images of the fractured surfaces of the H2F1 specimen broken in a tensile test.

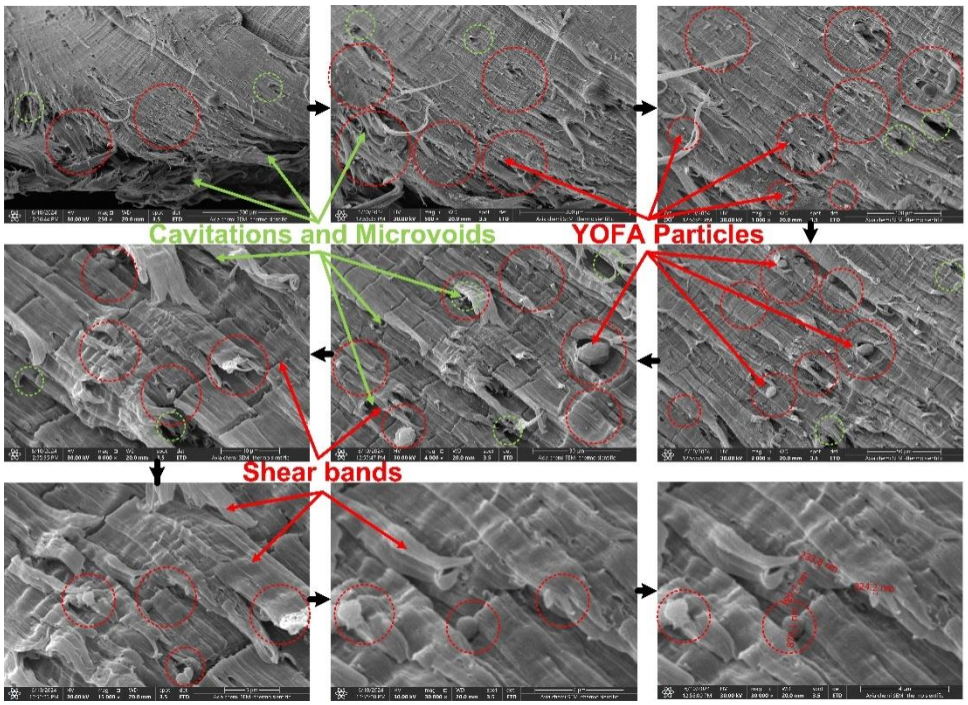

Figure 11. SEM images of the fractured surfaces of the H8F1 specimen broken in a tensile test.

  - Volume 19, Number 1 (ISSN 1995-6665)

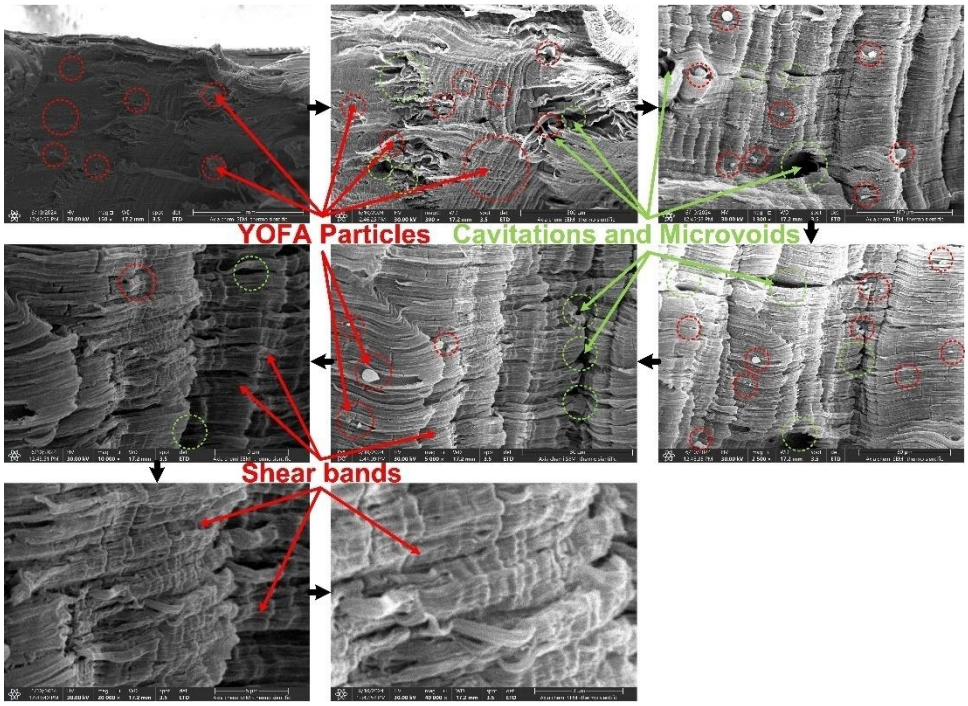

Figure 12. SEM images of the fractured surfaces of the H2F4 specimen broken in a tensile test.

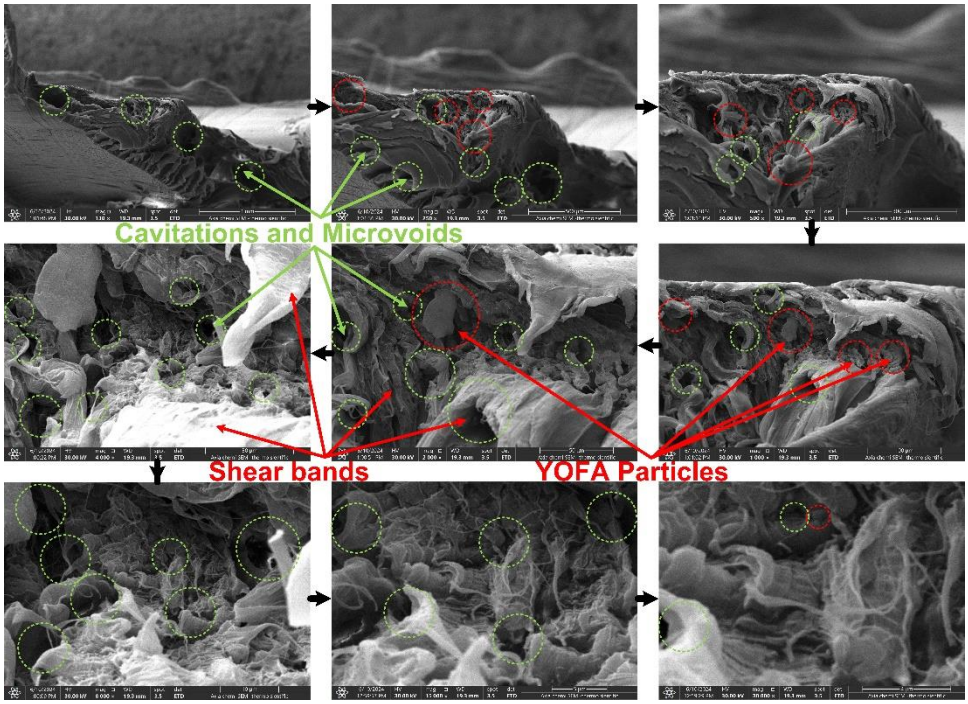

Figure 13. SEM images of the fractured surfaces of the H8F4 specimen broken in a tensile test.

3.2. Flexural properties

Figure 14 and Figure **15** clearly depict the correlation between the content and size of YOFA particles with the flexural strength and modulus, respectively, for the HDPE matrix composites. The flexural strength and modulus of the HDPE matrix composite for all particle sizes exhibit a notable increase with the escalating YOFA particle content, reaching a peak at 2 wt.%. Subsequently, these properties gradually reduce across all the composites. Moreover, an increase in YOFA particle size leads to a gradual decline in flexural strength and modulus for all concentrations of YOFA content. Compared with neat HDPE (NHD), the HDPE/YOFA composites with YOFA 1 and YOFA 2 particle sizes demonstrate higher flexural strength, whereas the flexural modulus is higher at all particle sizes. This behavior may be associated with the same factors mentioned above regarding tensile strength behavior. Composites containing 2 wt.% YOFA showed maximum improvement in flexural strength up to 21, 12, 10, and 7 % for YOFA 1, YOFA 2, YOFA 3, and YOFA 4, respectively, while improvement in flexural modulus up to 42.5, 21, 19.6, 17.7 % for YOFA 1, YOFA 2, YOFA 3, and YOFA 4, respectively.The observed improvement in

flexural properties can be attributed to the enhanced interfacial interaction between YOFA and the matrix polymer. Conversely, the increased flexural modulus of HDPE is primarily attributed to the heightened entanglement density of the HDPE matrix resulting from the presence of YOFA particles. Verma et al. [23] observed a similar trend, which improved the flexural strength of HDPE/FA composites by up to 5 wt.% FA content and then decreased it. This improvement behavior is a promising development in composite systems, where the reinforcing filler leads to increased modulus through the efficient transfer of stress from the HDPE matrix to the particles at the interface [38]. As per Satapathy et al. [29], the increased flexural strength and modulus increase indicate an enhancement in chain stiffness attributed to rigid FA particles.

Besides, the declining flexural strength and modulus behavior beyond 2 wt.% to 8 wt.% indicates that further investigation is necessary. This decline may be attributed to several reasons, which will delve into the following points:

1. Distribution Challenges: Increasing the amount of YOFA in a material raises the chances of particles clumping together. This clumping, caused by van der Waals forces, leads to an uneven spread within the HDPE matrix. These clumps of particles, also known as agglomerates, intensify stress in the material, making it easier for cracks to form and spread when the material is flexed.
2. Inherent Properties of YOFA:
   - Brittleness: The YOFA material mainly comprises brittle inorganic oxides and sulfites, as shown in Table 1. These brittle particles make the composite less flexible and tough when added to the HDPE material. This brittleness becomes more noticeable as the amount of YOFA in the material increases, directly affecting its flexural strength and modulus.
   - Mechanical Mismatch: The distinct variance in mechanical properties between the YOFA particles and the HDPE matrix results in stress concentrations at the interface, ultimately causing premature failure under flexural loading.
3. Microstructural Defects:
   - Void Formation: During the production of HDPE-YOFA composites, voids and micro-voids develop, particularly when the YOFA content is high. These voids diminish the effective load-bearing area and act as starting points for cracks, ultimately diminishing the flexural strength and modulus.
   - Stress Concentration: Irregularities and defects within the composite structure, especially around poorly bonded YOFA particles, act as stress concentrators, creating localized regions of high stress that can cause failure under bending loads.
4. Reduction in HDPE Content:
   - HDPE Continuity: As the YOFA concentration rises, the proportion of the HDPE matrix declines. The HDPE matrix is crucial for the composite's ductility and flexibility. A higher filler loading disrupts the continuity of the matrix, reducing the material's ability to deform under load and directly affecting flexural properties.
   - Mechanical Integrity: The HDPE matrix mainly provides toughness and flexibility to the composite. A lower HDPE content results in fewer beneficial properties to offset the brittle nature of the fly ash, leading to an overall decrease in flexural strength and modulus.

On the other hand, the smaller particle size of YOFA possesses high flexural properties compared with the larger particle size for all composite content. The enhanced flexural properties of HDPE are attributed to the higher exposure of smaller YOFA particles to the polymer matrix, owing to their greater surface area. This increases interfacial interaction between the YOFA particles and the HDPE matrix. Conversely, larger YOFA particles exhibit reduced specific surface area, leading to fewer bonding sites with the HDPE matrix. Consequently, the bond between the polymer matrix and the filler weakens, impeding efficient stress transfer and causing a decline in flexural strength and modulus. Additionally, the presence of larger YOFA particles in the HDPE matrix may function as stress concentrators, further compromising the material's properties. Under flexural load, these stress concentrators can initiate microcracks, propagating more easily than a composite with finer particles. The larger particles increase the likelihood of defects and voids, contributing to the initiation and growth of cracks and ultimately reducing the flexural properties.

3.3. Impact strength:

Figure 16 displays the correlation between the impact strength and the content and particle size of the YOFA content. As can be seen, the impact strength values decreased slightly and linearly with the increasing concentration and particle size of YOFA content in the HDPE matrix. Specifically, the reductions were -15.7%, -19%, -24.7%, and -29% for YOFA 1, YOFA 2, YOFA 3, and YOFA 4, respectively. The Izod impact resistance significantly decreases as filler concentration rises, irrespective of particle size. Moreover, a minor reduction in impact resistance accompanies larger particle sizes. The addition of YOFA particles to the polymer matrix results in the formation of stress concentrators, further diminishing impact resistance with higher YOFA content. The aggregation of YOFA also contributes to easier crack initiation, leading to composites with increased brittleness due to larger particle size and reduced impact strength [40], [41]. Finally, the deterioration behavior of Izod impact strength is attributed to the same reasons for the decline in the tensile and flexural strength mentioned above, which increases the concentration and particle size of the YOFA. Additionally, adding smaller particles improves the composite's capacity to disperse energy through plastic deformation and micro-cracking processes. On the other hand, larger particles impede these energy dissipation processes due to their size, which inhibits effective energy absorption and redistribution. This limitation in energy dissipation contributes to a noticeable reduction in impact strength. Smaller particles facilitate a more uniform and fine distribution within the HDPE matrix, ultimately enhancing the material's toughness. Conversely, larger particles disrupt this uniform dispersion, leading to an overall decrease in the

composite's toughness. Reduced toughness is directly linked to a diminished ability to absorb impact energy, thereby lowering the Izod impact strength. Satapathy et al. [29], [38] explained this decline in the impact strength in the case of FA-reinforced HDPE composites. As the content of filler improves, the material's elasticity reduces, thereby reducing the matrix's deformability and ability to absorb deformation energy. On the other hand, Kabir et al. [25] suggested that FA additions adversely affect the impact properties of HDPE/FA composites, resulting from the concentration of stress due to the FA particulates and the low toughness of fracture of the vitreous FA.

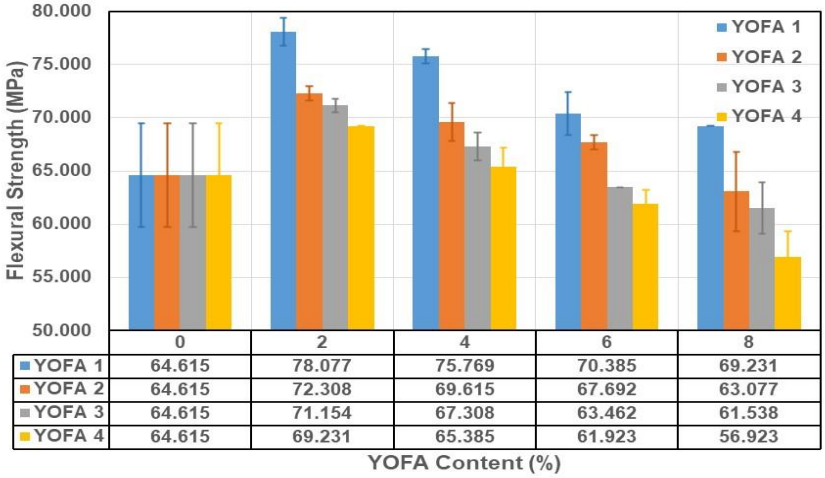

	0	2	4	6	8
YOFA 1	64.615	78.077	75.769	70.385	69.231
YOFA 2	64.615	72.308	69.615	67.692	63.077
YOFA 3	64.615	71.154	67.308	63.462	61.538
YOFA 4	64.615	69.231	65.385	61.923	56.923

Figure 14. Correlation between the flexural strength with the content and particle size of YOFA content.

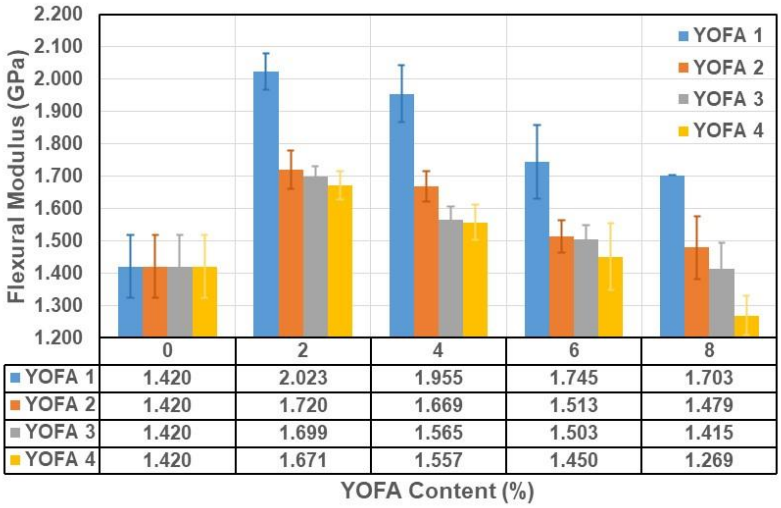

	0	2	4	6	8
YOFA 1	1.420	2.023	1.955	1.745	1.703
YOFA 2	1.420	1.720	1.669	1.513	1.479
YOFA 3	1.420	1.699	1.565	1.503	1.415
YOFA 4	1.420	1.671	1.557	1.450	1.269

Figure 15. Correlation between the flexural modulus with the content and particle size of YOFA content.

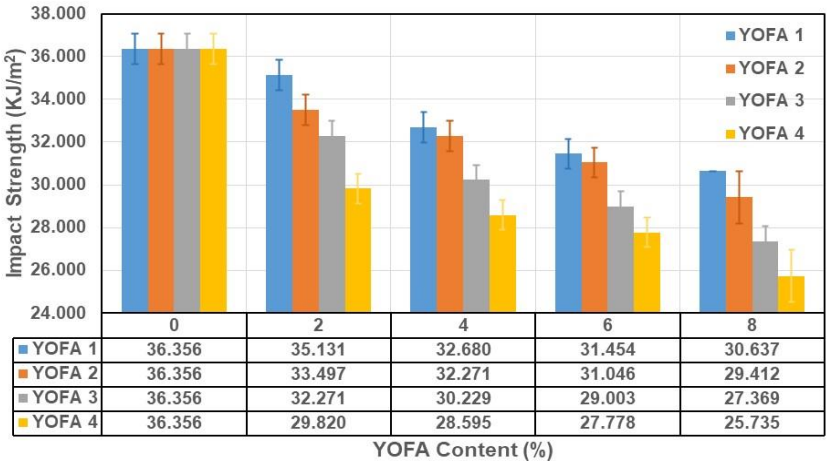

	0	2	4	6	8
YOFA 1	36.356	35.131	32.680	31.454	30.637
YOFA 2	36.356	33.497	32.271	31.046	29.412
YOFA 3	36.356	32.271	30.229	29.003	27.369
YOFA 4	36.356	29.820	28.595	27.778	25.735

Figure 16. Correlation between the Impact strength with the concentration and particle size of YOFA content.

3.4. Thermal analysis:

Figure 17 presents the TGA and DTA results of NHD, H2F1, H8F1, H2F4, and H8F4, respectively. These results give insight into the amount of weight lost during the decomposition process. The TGA/DTA curves display three different stages: stages I, II, and III. Stage I occurs from 25°C to 400°C and is primarily associated with the evaporation of moisture adsorbed on the surface of the polystyrene molecules in the samples. During this stage, minimal weight loss is observed for HDPE and HDPE/YOFA composite samples, indicating that environmental humidity has little influence on the properties of HDPE and HDPE-based composites. The primary stage (stage II) in the TGA/DTA curve represents the thermal decomposition of HDPE and HDPE/YOFA composites within the range of temperature 400–500°C, during which the most significant weight loss is observed. The substantial weight loss observed during this thermal decomposition process (stage II) is likely due to the primary chain pyrolysis and the release of aromatic substances resulting from the degradation of the ethylene component.

Figure 18shows the three essential temperatures and the amount of residue left as a function of NHD, H2F1, H8F1, H2F4, and H8F4, respectively, which are:

1. T onset: the temperature at the beginning of the thermal decomposition rate.
2. T max: the temperature at the highest thermal decomposition rate.
3. T complete: the temperature at the complete thermal decomposition rate.

These values indicate the composite thermal stability. As can be seen, the temperatures linearly increase with YOFA content up to 2 wt.%, which means higher stability. This shows a strong bond between the YOFA particles and the HDPE matrix at the interface, restricting the movement of the polymer segments near the interface. This analysis demonstrates that the composite thermal stability improves as the YOFA content increases up to 2 wt.%. The enhancement in thermal stability is due to the YOFA filler content modifying the mobility of the polymer molecular chains by adsorbing onto the surface of the filler particles. Moreover, the remarkable enhancement in mechanical properties can be attributed to the outstanding characteristics of the composites, as explored in the earlier sections of our study. Our findings highlight that composites incorporating a 2 wt.% YOFA content showcased the most pronounced improvements in mechanical properties. This enhancement can be attributed to the superior interfacial bonding between the matrix and the fillers. In contrast, the HDPE/YOFA composites with the largest YOFA particle size show lower thermal stability than those with smaller particle sizes. Other researchers [29], [38], also observed increased thermal stability for FA-filled HDPE matrices with various FA content. The barrier effect of the filler particles can explain the sudden increase in the temperature at which decomposition occurs. These particles slow down the polymer's volatilization process when its thermal decomposition at high temperatures, which in turn helps the composite material maintain its thermal stability. This can happen because the polymer chains stick to the surface of the filler particles, limiting their movement and preventing reactions that might cause the chains to rearrange or break. Besides, the amount of residue is higher at the concentration of YOFA particles up to 8 wt.% in HDPE matrix composites. In the TGA/DTA curve, the third part (stageIII) occurs from 500°C to 800°C, which indicates the samples' residue at the experiment's conclusion, as depicted in Figure 17. Analysis of the residual mass results reveals that pure HDPE (NHD) undergoes almost complete decomposition (residual mass 0.73%) during stage II of thermal decomposition. The residual mass in the composites is attributed to the presence of YOFA content, which was exclusively used during the preparation of the composites.

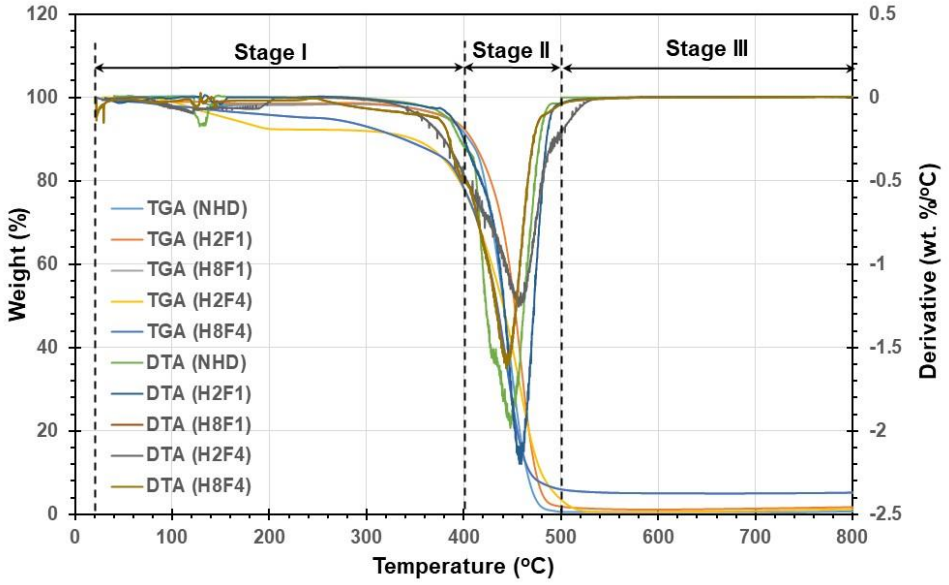

Figure 17. Correlation between the TGA/DTA curves with temperature for NHD, H2F1, H8F1, H2F4, and H8F4.

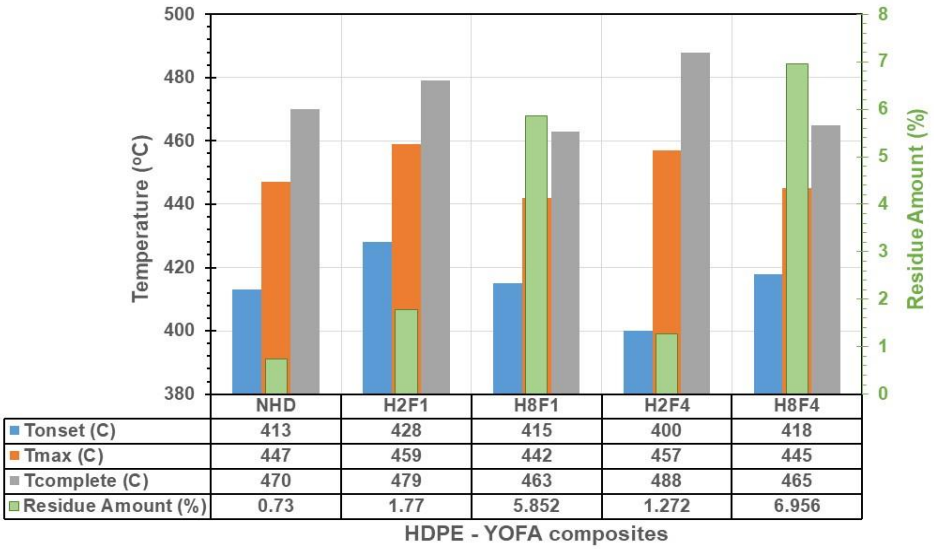

	NHD	H2F1	H8F1	H2F4	H8F4
Tonset (C)	413	428	415	400	418
Tmax (C)	447	459	442	457	445
Tcomplete (C)	470	479	463	488	465
Residue Amount (%)	0.73	1.77	5.852	1.272	6.956

HDPE - YOFA composites

Figure 18. Representation of different temperatures and residue amounts left from TGA/DTA curves.

4. Conclusions

This study introduced yellow oil fly ash (YOFA) as a novel reinforcement for HDPE matrix composites using the injection molding technique. The study aimed to analyze the effects of YOFA concentration and particle size on the mechanical and thermal properties of the HDPE/YOFA composites. These composites displayed relatively optimal tensile and flexural performance at 2 wt.% of YOFA with a 53-80 µm particle size. However, composites with the smallest YOFA particle size exhibit yield and tensile strengths higher than those of neat HDPE, up to 4 wt.% YOFA content. Nevertheless, the flexural strength of HDPE/YOFA composites with YOFA 1 and YOFA 2 particle sizes is higher compared to neat HDPE (NHD), while the flexural modulus is higher across all particle sizes. In contrast, the impact strength slightly declined with increasing YOFA content and particle size. Tensile fracture surface analysis shows thorough encapsulation of YOFA particles in the HDPE composite matrix. Besides, the TGA and DTA thermograms show that the HDPE/YOFA composites have optimum thermal stability with YOFA particles up to 2 wt.% and minimum particle size. In other words, optimal thermal stability fully corresponds to optimal flexural and tensile properties of the composites at 2 wt.% YOFA content and smaller particle size. These findings underscore the effectiveness of YOFA as a reinforcement material, enhancing both the thermal and mechanical properties of HDPE composites. The study provides a sustainable solution for industrial waste utilization with significant potential for applications in the construction, automotive, and packaging industries, where materials with superior strength and stability are crucial.

Disclosure statement

The authors declare that there is no conflict of interest.

References

[1] A.A. Abdul Rahman, O.J. Adeboye, A. Adebayo, M.R. Salleh, “Behaviour and Some Properties of Wood Plastic Composite Made from Recycled Polypropylene and Rubberwood,” Jordan Journal of Mechanical and Industrial Engineering, Vol. 17, No. 02, 2023, pp. 281–287, doi: 10.59038/jjmie/170211.

[2] K. M. P. Sadashiva. K, “Investigation on Mechanical and Morphological Characteristics of Ramie/Silk with Epoxy Hybrid Composite of Filler OMMT Nanoclay,” Jordan Journal of Mechanical and Industrial Engineering, Vol. 17, No. 02, 2023, pp. 289–296, doi: 10.59038/jjmie/170212.

[3] Priyank Lohiya, Alka Bani Agrawal, Alok Agrawal, Abhishek Kumar Jain, “Thermal Behaviour of Epoxy Composites Filled with Micro-sized LD Slag Particulates,” Jordan Journal of Mechanical and Industrial Engineering, Vol. 17, No. 04, 2023, pp. 645–651, doi: 10.59038/jjmie/170418.

[4] M. N. Alghamdi, “Performance for Fly Ash Reinforced HDPE Composites over the Ageing of Material Components,” Polymers (Basel), Vol. 14, No. 14, 2022, pp. 2913, doi: 10.3390/polym14142913.

[5] Sleem, Ahmad Abu, Mazen Arafeh, Sameh Al-Shihabi, Ruba Obiedat, and Yazan Al-Zain., “Glass-Reinforced Aluminum Matrix Composite: Synthesizes, Analysis, and Hardness and Porosity Modeling Using Artificial Neural Networks,” Jordan Journal of Mechanical and Industrial Engineering, Vol. 18, No. 03, 2024, pp. 509–519, doi: 10.59038/jjmie/180306.

[6] M. Cosnita, M. Balas, and C. Cazan, “The Influence of Fly Ash on the Mechanical Properties of Water Immersed All Waste Composites,” Polymers (Basel), Vol. 14, No. 10, 2022, pp. 1957, doi: 10.3390/polym14101957.

[7] D. Bryce, J. L. Thomason, and L. Yang, “Thermoset droplet curing performance in the microbond test,” Compos Interfaces, 2024, pp. 1–22,doi: 10.1080/09276440.2024.2337458.

[8] Hakmi, Tallal, Amine Hamdi, Aissa Laouissi, Hammoudi Abderazek, Salim Chihaoui, and Mohamed Athmane Yallese., “Mathematical Modeling Using ANN Based on k-fold Cross Validation Approach and MOAHA Multi-Objective Optimization Algorithm During Turning of Polyoxymethylene POM-C,” Jordan Journal of Mechanical and Industrial Engineering, Vol. 18, No. 01, 2024, pp. 179–190, doi: 10.59038/jjmie/180114.

[9] A. K. Maurya, R. Gogoi, S. K. Sethi, and G. Manik, "A combined theoretical and experimental investigation of the valorization of mechanical and thermal properties of the fly ash-reinforced polypropylene hybrid composites," Journal of Materials Science, Vol. 56, No. 30, 2021, pp. 16976–16998, doi: 10.1007/s10853-021-06383-2.

[10] V. K. , and U. KS. Vasu, "Empirical Analysis of Multiwalled Carbon Nanotube Deposition for Enhancing Mechanical and Tribological Characteristics in Aluminium-Based Metal Matrix Composites," Jordan Journal of Mechanical and Industrial Engineering, Vol. 17, No. 04, 2023, pp. 471–480,doi: 10.59038/jjmie/170402.

[11] A. K. Dan et al., "Prospective Utilization of Coal Fly Ash for Making Advanced Materials," in Clean Coal Technologies, Cham: Springer International Publishing, 2021, pp. 511–531. doi: 10.1007/978-3-030-68502-7_20.

[12] N. H. Mohd Nasir, F. Usman, E. L. Woen, M. N. M. Ansari, and A. B. M. Supian, "Microstructural and Thermal Behaviour of Composite Material from Recycled Polyethylene Terephthalate and Fly Ash," Recycling, Vol. 8, No. 1, 2023, pp. 11, doi: 10.3390/recycling8010011.

[13] Hany Mohamed Abdu, Sayed M. Tahaa, A.Wazeer, A.M.Abd El-Mageed, Moustafa M. Mahmoud, "Application of Taguchi Method and Response Surface Methodology on Machining Parameters of Al MMCs 6063-TiO2," Jordan Journal of Mechanical and Industrial Engineering, Vol. 17, No. 04, 2023, pp. 489–499, doi: 10.59038/jjmie/170404.

[14] M. S. Sreekanth, V. A. Bambole, S. T. Mhaske, and P. A. Mahanwar, "Effect of Particle Size and Concentration of Flyash on Properties of Polyester Thermoplastic Elastomer Composites," Journal of Minerals and Materials Characterization and Engineering, Vol. 08, No. 03, 2009, pp. 237–248,doi: 10.4236/jmmce.2009.83021.

[15] S. Chen, S. Xie, S. Guang, J. Bao, X. Zhang, and W. Chen, "Crystallization and Thermal Behaviors of Poly(ethylene terephthalate)/Bisphenols Complexes through Melt Post-Polycondensation," Polymers (Basel), Vol. 12, No. 12, 2020, pp. 3053,doi: 10.3390/polym12123053.

[16] S. Hwang et al., "Deciphering van der Waals interaction between polypropylene and carbonated fly ash from experimental and molecular simulation," Journal of Hazardous Materials, Vol. 421, 2022, pp. 126725, doi: 10.1016/j.jhazmat.2021.126725.

[17] M. N. Alghamdi, "Effect of Filler Particle Size on the Recyclability of Fly Ash Filled HDPE Composites," Polymers (Basel), Vol. 13, No. 16, 2021, pp. 2836,doi: 10.3390/polym13162836.

[18] N. Omair and M. Z. Intan Syaqirah, "Mechanical Properties of Recycled High-Density Polyethylene, Rice Husk Ash, and Fly Ash Composite Mixture," Journal of Innovation and Technology, Vol. 2022, No. 22, 2022, pp. 1–8.

[19] Singh, Saurabh Kumar, Pankaj Yadav, Sambhrant Srivastava, Amit Bhaskar, and Brihaspati Singh., "Laser Machining of Kevlar Polypropylene Composites: Effect of Continuous versus Modulated Wave Operational Mode," Jordan Journal of Mechanical and Industrial Engineering, Vol. 18, No. 03, pp. 2024, 455–460, doi: 10.59038/jjmie/180301.

[20] A. A. and U. E. Inyang. Victor, "Development and Properties Characterization of Polyethylene Based Composite Using Coconut Fiber," Jordan Journal of Mechanical and Industrial Engineering, Vol. 18, No. 02, 2024, pp. 287–295, doi: 10.59038/jjmie/180203.

[21] I. Ahmad and P. A. Mahanwar, "Mechanical properties of fly ash filled high density polyethylene," Journal of minerals and materials characterization and engineering, Vol. 9, No. 03, 2010, pp. 183.

[22] ASTM International, "Standard Test Method for Density (Relative Density) of Solid Pitch (Pycnometer Method)," 2017.

[23] P. Verma, A. Kumar, S. S. Chauhan, M. Verma, R. S. Malik, and V. Choudhary, "Industrially viable technique for the preparation of HDPE/fly ash composites at high loading: Thermal, mechanical, and rheological interpretations," Journal of Applied Polymer Science, Vol. 135, No. 11, 2018, pp. 459951, doi: 10.1002/app.45995.

[24] American Society for Testing and Materials, "ASTM D638: Standard Test Method for Tensile Properties of Plastics," in Book of ASTM Standards, Vol. 08.01, 2022.

[25] I. I. Kabir, C. C. Sorrell, M. R. Mada, S. T. Cholake, and S. Bandyopadhyay, "General model for comparative tensile mechanical properties of composites fabricated from fly ash and virgin/recycled high-density polyethylene," Polymer Engineering & Science, Vol. 56, No. 10, 2016, pp. 1096–1108, doi: 10.1002/pen.24342.

[26] ASTM International, "ASTM Standard D790-17 Standard Test Methods for Flexural Properties of Unreinforced and Reinforced Plastics and Electrical Insulating Materials," ASTM International, 2017.

[27] ASTM, "ASTM D 256 Standard Test Methods for Determining the Izod Pendulum Impact Resistance of Plastics," Annual Book of ASTM Standards, 2010.

[28] Z. Cao, M. Daly, L. M. Geever, I. Major, C. L. Higginbotham, and D. M. Devine, "Synthesis and characterization of high density polyethylene/peat ash composites," Composites Part B: Engineering, Vol. 94, 2016, pp. 312–321, doi: 10.1016/j.compositesb.2016.03.009.

[29] S. Satapathy and G. Bihari Nando, "Mechanical, dynamic mechanical, and thermal characterization of fly ash and nanostructured fly ash-waste polyethylene/high-density polyethylene blend composites," Polymer Composites, Vol. 37, No. 11, 2016, pp. 3256–3268, doi: 10.1002/pc.23524.

[30] R. N. Hwayyin and A. S. Ameed, "The Time Dependent Poisson's Ratio of Nonlinear Thermoviscoelastic Behavior of Glass/Polyester Composite.," Jordan Journal of Mechanical and Industrial Engineering, Vol. 16, No. 4, 2022.

[31] U. Atikler, D. Basalp, and F. Tihminlioğlu, "Mechanical and morphological properties of recycled high-density polyethylene, filled with calcium carbonate and fly ash," Journal of Applied Polymer Science, Vol. 102, No. 5, 2006, pp. 4460–4467, doi: 10.1002/app.24772.

[32] J. A. Jansen, "Characterization of Plastics in Failure Analysis," in Characterization and Failure Analysis of Plastics, 2023. doi: 10.31399/asm.hb.v11b.a0006933.

[33] P. A. O'Connell and G. B. McKenna, "Yield and Crazing in Polymers," in Encyclopedia of Polymer Science and Technology, 2004. doi: 10.1002/0471440264.pst463.

[34] S. Satapathy, A. Nag, and G. B. Nando, "Effect of electron beam irradiation on the mechanical, thermal, and dynamic mechanical properties of flyash and nanostructured fly ash waste polyethylene hybrid composites," Polymer Composites, Vol. 33, No. 1, 2012, pp. 109–119, doi: 10.1002/pc.22140.

[35] S. Bose and P. A. Mahanwar, "Effect Of Flyash On The Mechanical, Thermal, Dielectric,Rheological And Morphological Properties Of Filled Nylon 6," Journal of Minerals and Materials Characterization and Engineering, Vol. 03, No. 02, 2004, doi: 10.4236/jmmce.2004.32007.

[36] N. Chand, P. Sharma, and M. Fahim, "Correlation of mechanical and tribological properties of organosilane modified cenosphere filled high density polyethylene," Materials Science and Engineering: A, Vol. 527, No. 21–22, 2010, pp. 5873–5878,doi: 10.1016/j.msea.2010.06.022.

[37] E. P. Ayswarya, B. T. Abraham, and E. T. Thachil, "HDPE-ash nanocomposites," Journal of Applied Polymer Science, Vol. 124, No. 2, 2012, pp. 1659–1667,doi: 10.1002/app.35191.

[38] S. Satapathy, G. B. Nando, A. Nag, and K. V. S. N. Raju, "HDPE-Fly Ash/Nano Fly Ash Composites," Journal of

Applied Polymer Science, Vol. 130, No. 6, 2013, doi: 10.1002/app.39733.

[39] B. R. Bharath Kumar, M. Doddamani, S. E. Zeltmann, N. Gupta, M. R. Ramesh, and S. Ramakrishna, "Processing of cenosphere/HDPE syntactic foams using an industrial scale polymer injection molding machine," Materials & Design, Vol. 92, 2016, pp. 414–423,doi: 10.1016/j.matdes. 2015.12.052.

[40] A. K. Sharma and P. A. Mahanwar, "Effect of particle size of fly ash on recycled poly (ethylene terephthalate) / fly ash composites," International Journal of Plastics Technology, Vol. 14, No. 1, 2010, pp. 53–64, doi: 10.1007/s12588-010-0006-2.

[41] L. Morawski, "Plastics Engineering," Imagine, Vol. 6, No. 3, 1999, doi: 10.1353/imag.2003.0244.